5-1-2012

Thermal conductivity of bulk and thin-film silicon: A Landauer approach

Changwook Jeong
Birck Nanotechnology Center, Purdue University

Supriyo Datta
Birck Nanotechnology Center, Purdue University, datta@purdue.edu

Mark S. Lundstrom
Birck Nanotechnology Center, Purdue University, lundstro@purdue.edu

Jeong, Changwook; Datta, Supriyo; and Lundstrom, Mark S., "Thermal conductivity of bulk and thin-film silicon: A Landauer approach" (2012). *Birck and NCN Publications.* Paper 1201.
http://dx.doi.org/10.1063/1.4710993

AIP | Journal of Applied Physics

Thermal conductivity of bulk and thin-film silicon: A Landauer approach

Changwook Jeong, Supriyo Datta, and Mark Lundstrom

Citation: J. Appl. Phys. **111**, 093708 (2012); doi: 10.1063/1.4710993
View online: http://dx.doi.org/10.1063/1.4710993
View Table of Contents: http://jap.aip.org/resource/1/JAPIAU/v111/i9
Published by the AIP Publishing LLC.

Thermal conductivity of bulk and thin-film silicon: A Landauer approach

Changwook Jeong, Supriyo Datta, and Mark Lundstrom
Network for Computational Nanotechnology, Birck Nanotechnology Center, Purdue University, West Lafayette, Indiana 47907, USA

(Received 1 February 2012; accepted 31 March 2012; published online 3 May 2012)

The question of what fraction of the total heat flow is transported by phonons with different mean-free-paths is addressed using a Landauer approach with a full dispersion description of phonons to evaluate the thermal conductivities of bulk and thin film silicon. For bulk Si, the results reproduce those of a recent molecular dynamic treatment showing that about 50% of the heat conduction is carried by phonons with a mean-free-path greater than about 1 μm. For the in-plane thermal conductivity of thin Si films, we find that about 50% of the heat is carried by phonons with mean-free-paths shorter than in the bulk. When the film thickness is smaller than $\sim$0.2 μm, 50% of the heat is carried by phonons with mean-free-paths longer than the film thickness. The cross-plane thermal conductivity of thin-films, where quasi-ballistic phonon transport becomes important, is also examined. For ballistic transport, the results reduce to the well-known Casimir limit [H. B. G. Casimir, Physica **5**, 495–500 (1938)]. These results shed light on phonon transport in bulk and thin-film silicon and demonstrate that the Landauer approach provides a relatively simple but accurate technique to treat phonon transport from the ballistic to diffusive regimes. © *2012 American Institute of Physics*. [http://dx.doi.org/10.1063/1.4710993]

I. INTRODUCTION

Recent molecular dynamics (MD) simulations[2] have shown that in bulk silicon (Si) about 50% of the heat is carried by phonons with mean-free-paths (MFPs) greater than about 1 μm—a fact that is surprising and that the authors of Ref. 2 could not explain with a simple, Callaway model with Debye approximation.[3] These results raise similar questions about heat transport in thin Si films. In this paper, we show that a simple Landauer model, essentially a Callaway model with full phonon dispersion, accurately reproduces the results of Ref. 2. We also show that the same model describes the in-plane thermal conductivity of silicon thin films and find that about 50% of the heat is carried by phonons with mean-free-paths shorter than in the bulk. When the film thickness is smaller than $\sim$0.2 μm, 50% of the heat is carried by phonons with mean-free-paths longer than the film thickness. Finally, we apply the technique to cross-plane thermal transport in Si. The results shed light on thermal transport in thin Si films and demonstrate that the Landauer approach provides a simple and accurate treatment of lattice thermal conductivity that is useful for analyzing experiments and for designing materials and structures.

The findings of Minnich *et al.*[2] for bulk Si raise questions about heat conduction in thin Si films and how the heat is carried by phonons with different MFPs. In silicon on insulator (SOI) films, it is well-known that the in-plane thermal conductivity decreases as the film thickness decreases due to the increasing importance of surface roughness scattering.[4–7] The influence of surface roughness is usually modeled by using either a constant[5–9] or frequency-dependent[4,10] specularity parameter, p, representing the probability of specular phonon boundary scattering. As an example, for perfectly diffusive scattering $p = 0$ and for perfectly specular scattering $p = 1$. The quantitative comparison between the in-plane thermal conductivities with constant and frequency-dependent p suggested that the frequency-dependent model provides a more accurate description for the in-plane thermal conductivity.[11] We show in this paper that with the addition of a model for surface roughness scattering, the Landauer model used for bulk Si also accurately describes in-plane thermal transport. We then use the model to address the question raised by the authors of Ref. 2: "How do phonons with various mean-free-paths contribute to thermal conduction in thin Si films?"

The measured cross-plane thermal conductivity of thin Si films has been found to be even lower than the in-plane thermal conductivity.[12] In some models,[13–15] the reduction in cross-plane thermal conductivity is modeled with the Boltzmann transport equation (BTE) by including a phonon-boundary scattering time (τ_b), which is assumed to be equal to the average time between "boundary scattering events:" $\tau_b = L/(2\upsilon)$, where L is the length of the conductor and υ the group velocity. Ballistic phonon transport (i.e., no phonon scattering within thin film), which becomes important in cross-plane transport is typically described by an equation of phonon radiative transport (EPRT),[16] which has been developed based on the Boltzmann equation and the analogy between phonons and photons. In the ballistic limit and with the Debye approximation, the EPRT yields a familiar blackbody radiation law for phonons,[17] $q = \sigma(T_H^4 - T_C^4)$, where σ is the Stefan-Boltzmann constant for phonons. This result has also been derived by Casimir,[1] who treated a perfectly diffusive surface ($p = 0$) as if it absorbed all phonons incident upon it and reemitted them at a rate depending on the absolute temperature of the surface according to the theory of blackbody radiation. We will show in this paper that the same Landauer approach used to describe diffusive phonon transport can be simply extended to accurately describe ballistic and quasi-ballistic transport.

The Landauer approach is widely used to treat ballistic electron[18] and phonon[19,20] transport in nanostructures. As recently shown for electrons[21] and phonons,[22] the method can also be applied to diffusive transport in bulk materials. The approach reduces to the BTE for diffusive transport but is more physically transparent and also provides some computational advantages. Section II presents a brief summary of the formalism for phonon transport as discussed in detail in Ref. 22. In Sec. III, results for the thermal conductivity of bulk Si are presented and compared to recent molecular dynamics simulations. In Sec. IV, the in-plane and cross-plane thermal conductivities are discussed. Sections III and IV also illustrate a general approach for extracting a well-defined mean-free-path for phonons from measured thermal conductivity data. In Sec. V, we discuss the ballistic limit of phonon transport and relate the Landauer expressions to the well-known Casimir formula.[1] Finally, our conclusions are summarized in Sec. VI.

II. APPROACH

This paper is an application of the approach presented in Ref. 22. The Landauer formula for heat current (I_Q) is expressed as

$$I_Q = \frac{1}{h}\int_0^\infty d(\hbar\omega)(T_{ph}M_{ph})\hbar\omega(n_1 - n_2), \tag{1a}$$

where T_{ph} is the transmission at a given energy $\hbar\omega$, M_{ph} is the number of conducting channels at a given energy, and n_1 and n_2 are Bose-Einstein distributions for the two contacts across which heat flows.[18] The transmission T_{ph} is given as[18]

$$T_{ph} = \lambda_{ph}(\omega)/(L + \lambda_{ph}(\omega)), \tag{1b}$$

where $\lambda_{ph}(\omega)$ is the mean-free-path for backscattering and L the length of the conductor. Equation (1a) applies to the ballistic limit ($L \ll \lambda_{ph}(\omega)$) for which $T_{ph} = 1$, the quasi-ballistic regime ($L \sim \lambda_{ph}(\omega)$) for which $T_{ph} = \lambda_{ph}(\omega)/(L + \lambda_{ph}(\omega))$ as well as to the diffusive limit ($L \gg \lambda_{ph}(\omega)$) for which $T_{ph} = \lambda_{ph}(\omega)/L$. In the diffusive limit, it was shown that the Landauer expression for lattice thermal conductivity is essentially equivalent to the conventional expression from BTE.[22] Note that the product $T_{ph}M_{ph}$ is proportional to the well-known "transport distribution" for electrons.[23]

For a small temperature gradient (ΔT), thermal conductance ($K_{ph} = I_Q/\Delta T$) is

$$K_{ph} = \left(\frac{k_B^2 T_L \pi^2}{3h}\right)\int_0^{+\infty} d(\hbar\omega)(T_{ph}M_{ph})W_{ph}, \tag{2a}$$

where $k_B^2 T_L \pi^2/3h$ is the quantum of thermal conductance with TL being the lattice temperature and W_{ph} is a "window function" given by[22]

$$W_{ph}(\hbar\omega) = \frac{3}{\pi^2}\left(\frac{\hbar\omega}{k_B T_L}\right)^2\left(-\frac{\partial n_0}{\partial(\hbar\omega)}\right). \tag{2b}$$

The integral of the window function, W_{ph}, from 0 to ∞ is 1, just like the derivative of the Fermi function $(-\partial f_0/\partial E)$ appearing in the expression for electrical conductivity. The thermal conductance, Eq. (2a), can be also expressed as

$$K_{ph} = \left(\frac{k_B^2 T_L \pi^2}{3h}\right)\langle M_{ph}\rangle\langle\langle T_{ph}\rangle\rangle, \tag{2c}$$

where the average $\langle X\rangle$ for any quantity X is defined as $\langle X\rangle \equiv \int X W_{ph} d(\hbar\omega)$ while the average $\langle\langle X\rangle\rangle$ is defined as $\langle MX\rangle/\langle M\rangle$. From Eq. (2c), the expressions for the lattice thermal conductivity, $\kappa_{ph} = K_{ph}(L/A)$, can be expressed as

$$\kappa_{ph} = \left(\frac{k_B^2 T_L \pi^2}{3h}\right)\langle M_{ph}/A\rangle\langle\langle\lambda_{ph}\rangle\rangle_{eff}, \tag{3a}$$

where A is the cross-sectional area of the conductor and $\langle\langle\lambda_{ph}\rangle\rangle_{eff}$ is the effective MFP given as

$$\langle\langle\lambda_{ph}\rangle\rangle_{eff} = \langle\langle T_{ph}\rangle\rangle L = \langle\langle(\lambda_{ph}^{-1} + L^{-1})^{-1}\rangle\rangle. \tag{3b}$$

From Eq. (2c), the ballistic thermal conductance per area K_{ph_BAL}/A can be defined as

$$K_{ph\_BAL}/A = \left(\frac{k_B^2 T_L \pi^2}{3h}\right)\langle M_{ph}/A\rangle, \tag{3c}$$

so the thermal conductivity is expressed as

$$\kappa_{ph} = (K_{ph\_BAL}/A)\langle\langle\lambda_{ph}\rangle\rangle_{eff}. \tag{3d}$$

Since $\langle M_{ph}\rangle$ and K_{ph_BAL}/A can be readily obtained from the bandstructure, the $\langle\langle\lambda_{ph}\rangle\rangle_{eff}$ can be estimated by taking the ratio of measured κ_{ph} to the K_{ph_BAL}/A. Note that Eqs. (3a) and (3b) holds for all transport regimes. In the ballistic limit, $L \ll \lambda_{ph}$, $\langle\langle\lambda_{ph}\rangle\rangle_{eff} = L$ and in the diffusive limit, $L \gg \lambda_{ph}$, $\langle\langle\lambda_{ph}\rangle\rangle_{eff} = \langle\langle\lambda_{ph}\rangle\rangle$ with $\langle\langle\lambda_{ph}\rangle\rangle$ being the average MFP in the diffusive limit. In the quasi-ballistic limit, the appropriate effective MFP is given by Eq. (3b).

It was shown in Ref. 22 that given an accurate phonon dispersion, $M_{ph}(\omega)$ can be readily computed by a simple numerical technique—the "band counting" method. To evaluate $M_{ph}(\omega)$ in this work, a full band description of phonon dispersion was obtained from the Tersoff[24] interatomic pair potential model within the General Utility Lattice Program (GULP).[25] Then it is straightforward to compute K_{ph_BAL}/A.

III. BULK THERMAL CONDUCTIVITY

In this section, the phonon thermal conductivity of bulk Si will be evaluated and compared to a recent MD calculation.[2] Figure 1(a) displays the energy-resolved M_{ph}, λ_{ph}, and W_{ph} at 300 K for bulk Si. Note that the entire phonon dispersion participates in conduction since W_{ph} is almost constant. This is in sharp contrast to the case of electrons, in which the important energies are near the bottom of the band. The ballistic thermal conductance, K_{ph_BAL}, is readily evaluated from Eq. (3c). By comparing K_{ph_BAL} to the measured conductivity, κ_{ph},[26] the average MFP, $\langle\langle\lambda_{ph}\rangle\rangle$, is readily extracted from Eq. (3d). The results in Fig. 1(b) show that $\langle\langle\lambda_{ph}\rangle\rangle \simeq 135$ nm at $T = 300$K. (As will be discussed in Sec. V, when comparing this result to the conventional mean-free-path, l_{ph}, it is important to remember that the Landauer mean-free-path (or mean-free-path for backscattering) is 4/3 times longer.)[22]

To examine how heat is conducted by phonons with different mean-free-paths, we need expressions for the spectral phonon mean-free-path for backscattering,[22]

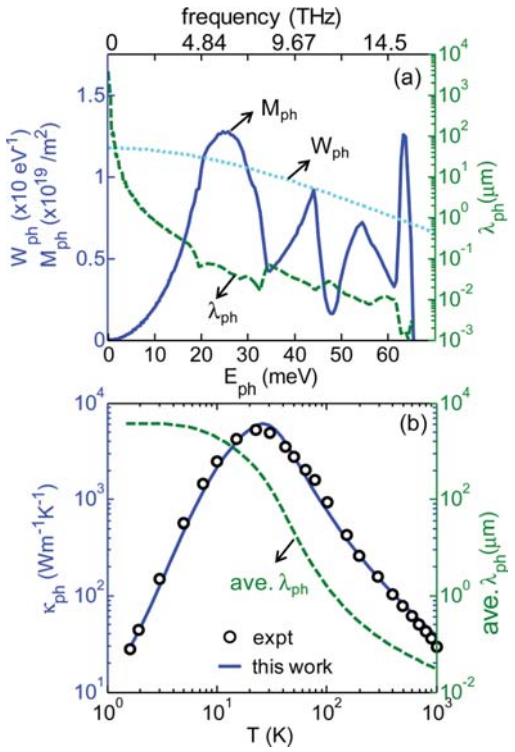

FIG. 1. (a) For bulk Si, energy-resolved number of conducting channels (M_{ph}), window function (W_{ph}), and the mean-free-path for backscattering (λ_{ph}) are plotted at 300 K. Note that the entire spectrum of M_{ph} participates in conduction since W_{ph} is almost constant. The mean-free-path shows that low-energy acoustic phonons have long λ_{ph} since they do not suffer a lot from umklapp scattering. The spectral λ_{ph} are calculated based on the relaxation time approximation for umklapp scattering,[27] point defect scattering,[28] and crystalline boundary scattering.[26] (b) The thermal conductivity κ_{ph}(left axis) and the average MFP $\langle\langle\lambda_{ph}\rangle\rangle$ (right axis) are plotted as a function of temperature. Experimental results are obtained from Ref. 26. Good agreement between calculation and experiment is observed.

$$\lambda_{ph}(\omega) = (4/3)\upsilon_{ph}(\omega)\tau_{ph}(\omega) = (4/3)l_{ph}(\omega), \qquad (4)$$

where $\upsilon_{ph}(\omega)$is the spectral phonon group velocity at frequency ω, $\tau_{ph}(\omega)$ the phonon momentum relaxation time, and $l_{ph}(\omega) = \upsilon_{ph}(\omega)\tau_{ph}(\omega)$. For $\tau_{ph}(\omega)$, the relaxation time approximation (RTA) is used for umklapp scattering,[27] point defect scattering,[28] and crystalline boundary scattering rates:[26] $\tau_u^{-1} = B\omega^2 T e^{-C/T}$, $\tau_d^{-1} = D\omega^4$, and $\tau_b^{-1} = \langle\upsilon(\omega)\rangle/(F \cdot l)$, respectively. Typical parameters to fit the κ_{ph} vs. T for bulk Si are used:[22] $B = 2.8 \times 10^{-19}$ s/K, $C = 140$ K, $F = 0.4$, and $l = 7.16 \times 10^{-3}$ m. Parameter $D = 1.32 \times 10^{-45}$ s^3 is analytically determined from the isotope concentration, so the value given in Ref. 26 is used for bulk Si. Figure 1(b) shows that the resulting fit is excellent. Figure 2 shows the cumulative distribution function of thermal conductivity as a function of energy with and without scattering. It can be seen that all energy channels contribute to the ballistic thermal conductance. When scattering is included, however, high energy channels contribute very little to κ_{ph} because high energy phonons have very short MFPs.

To find how the heat is carried by phonons with different MFPs, the spectral analysis (cumulative κ_{ph} vs. λ_{ph}) is presented in Fig. 3. Note that the scattering parameters are

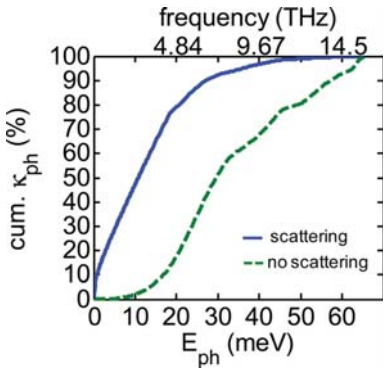

FIG. 2. The cumulative thermal conductivity, κ_{ph}, as a function of energy is plotted for diffusive (scattering) and ballistic (no scattering) cases. For the ballistic case, all energy channels equally contribute to κ_{ph}. With scattering, low-energy channels mainly contribute to κ_{ph} because high-energy phonons have very short mean-free-paths.

adjusted to match measured κ_{ph} vs. T (Fig. 1(b)) rather than to obtain the same MFP distribution as the MD calculations. Our results obtained from full phonon dispersion (blue solid line) are in good agreement with the recent MD simulations[2]—~50% of the heat conduction is attributed to phonons with MFP >~1 μm. The reason is that the phonons with MFP > ~1 μm are low-energy acoustic phonons near the Brillouin zone center which do not suffer a lot from umklapp scattering, which compensates for the fact that there is a small percentage of low energy channels. As shown in Fig. 1(b), the average MFP for bulk Si ($\langle\langle\lambda_{ph}\rangle\rangle = \kappa_{ph}/(K_{ph\_BAL}/A)$) is about 0.135 μm at room temperature. Therefore, the commonly used average MFP does not give a clear picture of which phonons carry the heat since the $\langle\langle\lambda_{ph}\rangle\rangle$ includes a significant number of high energy modes with very small MFPs.

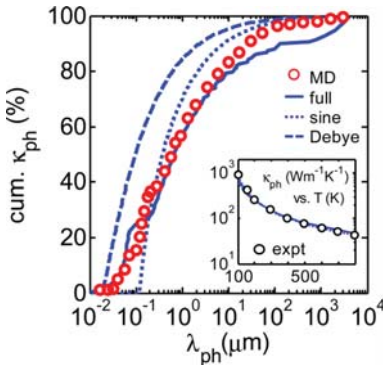

FIG. 3. We plot the computed cumulative thermal conductivity (κ_{ph}) as a function of the MFP for backscattering (λ_{ph}) using three different phonon dispersion models: full phonon dispersion, a sine-type dispersion, and a Debye model. The computed results are compared to the MD simulations obtained from Ref. 2. The MD simulation is plotted while taking into account the difference between a conventional MFP for scattering (l_{ph}) and the MFP for backscattering, i.e., $\lambda_{ph} = (4/3)l_{ph}$. Our results with full phonon dispersion (solid line) is in good agreement with the recent MD simulations,[2] which showed ~50% of the heat conduction is attributed to phonons with MFP >~1 μm. The MFP distribution is not correctly predicted by a simple sine-type dispersion model (dotted line) or a Debye model (dashed line). Inset: Computed thermal conductivity κ_{ph} vs. temperature is plotted for the three phonon dispersion models and is compared to experiment.[26] Note that regardless of the phonon dispersion model used, we can fit well the experimental data by adjusting scattering parameters.

To illustrate the effect of phonon dispersion model, two simple approximations of phonon dispersion are assumed. The first is a Debye model, $\omega = \upsilon_s k$, where υ_s is sound velocity and k is a wave vector, and the second is a sine-type dispersion model, $\omega = \omega_0 \sin(\pi k/2k_0)$,where ω_0 is the maximum phonon frequency and k_0 is the Debye cutoff wave vector.[29] As shown in the inset of Fig. 3, κ_{ph} vs. temperature computed from the two simple models almost overlap with the results of full phonon dispersion and match well the measured conductivity. But this requires an increase in the B parameter for umklapp scattering by a factor of 4.5 for the Debye model and a factor of 3 for the sine-type model. It can be clearly seen that while the simple phonon models can fit the measured thermal conductivity by adjusting fitting parameters, the MFP distribution of the simple models does not agree well with that of MD simulation. Thus, the question of how phonons with different MFPs carry the heat, which is important to know when designing thermoelectric devices is not correctly addressed by the simple phonon models.

IV. IN-PLANE AND CROSS-PLANE THERMAL CONDUCTIVITIES FOR THIN FILMS

Having verified that a simple Landauer model with full phonon dispersion accurately reproduces the results of MD simulations,[2] we turn next to heat transport in thin Si films. For thin Si films, phonon boundary scattering significantly influences the thermal conductivity. In this section, phonon thermal conductivity of thin Si film layers along the in-plane and the cross-pane direction will be evaluated as a function of Si layer thickness.

For in-plane thermal conduction in thin films, we consider the surface roughness of boundaries with a frequency-dependent specularity parameter. The scattering time reduction due to boundary scattering in the thin film has been examined by a solution of the BTE (Refs. 4 and 30) and the corresponding MFP of thin film ($\lambda_{ph,thin}$) compared to that of bulk Si ($\lambda_{ph,bulk}$) was given as

$$\lambda_{ph,thin}(\omega) = \lambda_{ph,bulk}(\omega)\left[1 - \frac{3(1-p)}{2\delta}\int_1^\infty \left(\frac{1}{t^3} - \frac{1}{t^5}\right) \times \frac{1-\exp(-\delta t)}{1-p\exp(-\delta t)}\,dt\right], \tag{5a}$$

where $\delta = (4/3)d_{Si}/\lambda_{ph,bulk}$ with d_{Si} being the thickness of Si thin film, and the specularity parameter p is given by[10]

$$p = \exp\left(-\frac{16\pi^3\eta_{SOI}^2}{\Lambda_{ph}^2}\right), \tag{5b}$$

where Λ_{ph} is the phonon wavelength and η_{SOI} is the surface roughness which was estimated to be between 0.2 and 1 nm for SOI wafers.[31] To consider the impact of additional imperfections associated with the SOI wafers such as point defects, stacking faults, and dislocations, we use an approximate formula since it is not clear which type of defect is dominant. The same point defect scattering rate formula used for bulk Si ($\tau_d^{-1} = D\omega^4$) was used except that the prefactor, D, for SOI film is adjusted to fit the experimental thermal conductivity data of SOI film, yielding that the D for SOI film is 2× larger than D for bulk Si. (Note that for bulk Si we used the parameter $D = 1.32 \times 10^{-45}$ s^3 analytically determined from the isotope concentration.)[28] Assuming that the length of conductor, L, is much greater than $\lambda_{ph}(\omega)$, transport is diffusive and $T_{ph} = \lambda_{ph}(\omega)/L$ in Eq. (2a). For these calculations, we retain the bulk phonon dispersions. The results are shown in Fig. 4. Previous experimental data are in good agreement with the calculations, and considering point defects produces a better fit to thicker Si layers in SOI.

Next, we examine the cross-plane phonon thermal conductivity of thin Si film layers. For cross-plane thermal transport in thin films of thickness less than ~1 μm, quasi-ballistic transport becomes important. Therefore, the assumption of diffusive transport no longer holds. The cross-plane thermal conductivity is conventionally computed with the BTE by including a phonon-boundary scattering time. For example, $\tau_b = L/(2\upsilon)$ (Refs. 13–15) is commonly used, but the physical significance is unclear. In contrast to the previous work, we have included only scattering processes within the thin film—no interface resistances are considered. In a Landauer picture, we are assuming ideal reflection-less contacts at the top and bottom of the film, so our calculations will provide an upper limit that does not consider the interface resistances that may occur in practice. For the transmission, the expression, $T_{ph} = \lambda_{ph}(\omega)/(L + \lambda_{ph}(\omega))$, is used to describe quasi-ballistic transport.

Figure 4 shows our calculation of the cross-plane thermal conductivity which is defined as $\kappa_{ph} = K_{ph}(L/A)$ compared to a recent experimental observation.[12] In agreement with the one available measurement,[12] our calculations show a much reduced thermal conductivity in the cross-plane. This result occurs even though we have not included possible interface resistances and can be understood from Eq. (3a). In the ballistic limit, the effective mean-free-path approaches the thickness of the film. Note that a better fit for the cross-plane measurement could be obtained by increasing the parameter, D, in the point defect scattering rate formula (we

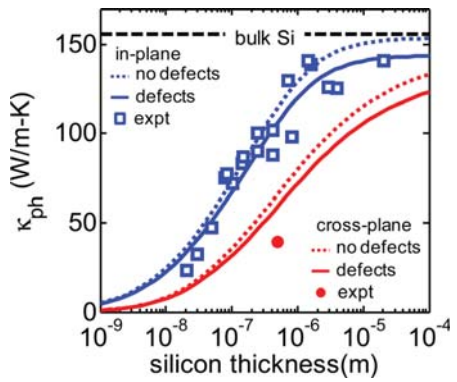

FIG. 4. Thermal conductivity (κ_{ph}) vs. silicon layer thickness at room temperature is plotted. In-plane experimental data[4–7] and calculations are shown by open squares and blue lines, respectively. For our calculations, a surface roughness of 0.5 nm is used, which is a typical value for SOI wafers. We assume that the point defect scattering rate for SOI wafer is 2× larger than that of bulk Si. The results with the point defects (blue solid line) give a better fit for thicker Si layers. The cross-plane experimental data[12] and calculations are shown by filled circle and red lines, respectively. It is assumed that the $M_{ph}(\omega)$ for the thin film is the same as that for bulk Si.

used the same D as for the in-plane calculation, 2× larger than D for bulk Si), but the comparison to experiment is clouded by uncertainties in possible interface resistances. Nevertheless, the calculation shows the reduction in thermal conductivity that should be expected for the thin film itself.

Next, we turn to the question of which phonons play the dominant role in the heat conduction in thin films. Figure 5 is a plot of $\lambda_{50\%}$ and $\langle\langle\lambda_{ph}\rangle\rangle_{eff}$ vs. thickness of thin Si films at room temperature along the in-plane and the cross-plane transport directions. Here, $\lambda_{50\%}$ is the MFP at which the cumulative κ_{ph} is equal to 50%, and the effective MFP, $\langle\langle\lambda_{ph}\rangle\rangle_{eff}$, is extracted according to Eq. (3d). The cross-plane direction displays about 2× smaller $\lambda_{50\%}$ and $\langle\langle\lambda_{ph}\rangle\rangle_{eff}$ than the in-plane direction. It can be also seen that $\langle\langle\lambda_{ph}\rangle\rangle_{eff}$ is always less than $\lambda_{50\%}$ for the same reason as for the bulk—$\langle\langle\lambda_{ph}\rangle\rangle_{eff}$ places too much emphasis on the high energy modes with very small MFPs. However, the difference between $\langle\langle\lambda_{ph}\rangle\rangle_{eff}$ and $\lambda_{50\%}$ decreases as the thickness of the thin film decreases. This occurs for both in-plane and cross-plane conduction but for different reasons. For cross-plane conduction, as the thickness of thin films (i.e., L in Eq. (1b)) decreases, the transmission T_{ph} in Eq. (1b) for phonons with short MFPs increases more rapidly than that for phonons with large MFPs. This results in a decrease of $\lambda_{50\%}$. For in-plane conduction, low-energy acoustic phonons, which have large MFPs ($\lambda_{ph} > \sim 1\ \mu$m) leading to the large $\lambda_{50\%}$ values in the bulk, suffer a lot from boundary scattering in thin films with thickness $<1\ \mu$m, and therefore, the $\lambda_{50\%}$ decreases rapidly with film thickness. Finally, we note that for the in-plane direction, about 50% of the heat conduction is carried by phonons with a mean-free-path greater than the thickness of the thin film when the thickness is smaller than $\sim 0.2\ \mu$m.

V. DISCUSSION

So far, we have applied the Landauer approach to diffusive transport in bulk materials and thin films along the in-plane direction as well as to quasi-ballistic transport in thin films along the cross-plane direction. Although the BTE with an additional boundary scattering (τ_b) succeeds in modeling, the bulk and thin film experiments, including τ_b, cannot accurately describe the ballistic limit (i.e., the Casimir limit, $q = \sigma(T_H^4 - T_C^4)$) for which Majumdar used the EPRT.[16] In this section, we show that the Landauer approach reduces to the Casimir limit under the appropriate conditions. We also relate the MFP for backscattering in the Landauer model to the commonly used MFP for scattering and discuss some limitations of the Landauer approach.

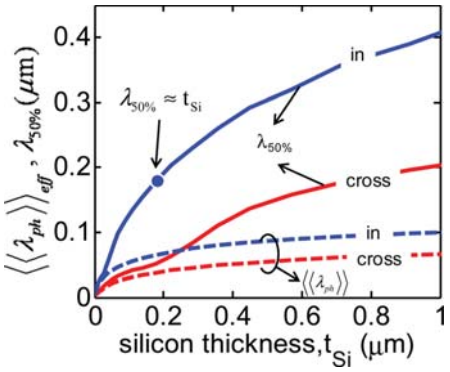

FIG. 5. Along the in-plane (in) and the cross-plane (cross) transport directions, $\lambda_{50\%}$and $\langle\langle\lambda_{ph}\rangle\rangle_{eff}$ are plotted as a function of the thickness of the thin Si films at room temperature. Here, $\lambda_{50\%}$ is the MFP at which the cumulative thermal conductivity (κ_{ph}) is equal to 50%, and the effective MFP, $\langle\langle\lambda_{ph}\rangle\rangle_{eff}$, is obtained from Eq. (3d). The cross-plane direction displays about 2× smaller $\lambda_{50\%}$ and $\langle\langle\lambda_{ph}\rangle\rangle_{eff}$ than the in-plane direction. $\langle\langle\lambda_{ph}\rangle\rangle_{eff}$ is always less than $\lambda_{50\%}$ since $\langle\langle\lambda_{ph}\rangle\rangle_{eff}$ places too much emphasis on the high energy modes with very small MFPs. Note that for the in-plane direction, about 50% of the heat conduction is carried by phonons with a mean-free-path greater than the thickness of the thin film when the thickness is smaller than $\sim 0.2\ \mu$m (blue symbol).

In the ballistic limit ($T_{ph} = 1$) and at a temperature much lower than the Debye temperature where $M_{ph}(\omega)$ is given as $M_{ph}(\omega) = A(3\omega^2/4\pi\upsilon_s^2)$ with υ_s being the velocity of sound. The heat flux (q) can be expressed from Eq. (1a) for a small temperature gradient (ΔT) as

$$q = \frac{I_Q}{A} = \frac{1}{h}\int_0^\infty d(\hbar\omega)\left(\frac{3\omega^2}{4\pi\upsilon_s^2}\right)\hbar\omega\left(\frac{dn}{dx}\frac{\partial x}{dT}\Delta T\right), \tag{6a}$$

where $n = 1/(e^x - 1)$ and $x \equiv \hbar\omega/k_BT$. Using $\int_0^\infty x^4(-dn/dx)dx = 4\pi^4/15$, the heat flux of Eq. (6a) is given as

$$q = \sigma\Delta(T^4), \tag{6b}$$

where $\sigma = \pi^2k_B^4/40\hbar^3\upsilon_s^2$ is the Stefan-Boltzmann constant for phonons.[17] This result shows that the Landauer approach correctly reduces to the Casimir result in the ballistic limit with the Debye approximation. Majumdar[16] showed that the Casimir limit can be also obtained from the EPRT and that the use of the Fourier law causes significant errors for conduction across the film. The EPRT, however, does not accurately predict the thermal conductivity reduction for both the in-plane and the cross-plane conduction of Si thin films[13] due to the gray approximation. Finally, note that more generally, for temperatures above the Debye temperature, the ballistic heat flux is $q = (K_{ph\_BAL}/A)\Delta T$, where the ballistic thermal conductance is given by Eq. (3c).

It was also shown from the EPRT (Ref. 16) with the gray approximation that the Fourier law can be used for all transport regimes if the effective mean-free-path for scattering, $\langle\langle l_{ph}\rangle\rangle_{eff}$, is used instead of the commonly used average MFP for scattering $\langle\langle l_{ph}\rangle\rangle$. According to Eq. (44) in Ref. 16

$$\langle\langle l_{ph}\rangle\rangle_{eff} = \frac{\langle\langle l_{ph}\rangle\rangle}{1 + (4/3)(\langle\langle l_{ph}\rangle\rangle/L)}, \tag{7a}$$

where the $\langle\langle l_{ph}\rangle\rangle$ is the average MFP for scattering that can be obtained from a classical kinetic theory (i.e., $\kappa_{ph} = (1/3)C_V\upsilon_s\langle\langle l_{ph}\rangle\rangle$ with C_V being the specific heat). A physical interpretation of Eq. (7a), however, was not given: For example, where does the value of 4/3 in the denominator come from? We can easily show that Eq. (7a) follows directly from Eq. (3b) of the Landauer approach. Using Eq. (4) in Eq. (7a) to convert from MFP to MFP for backscattering, we find

$$\langle\langle\lambda_{ph}\rangle\rangle_{eff} = \left(\frac{1}{\langle\langle\lambda_{ph}\rangle\rangle} + \frac{1}{L}\right)^{-1}, \tag{7b}$$

which is precisely the Landauer result if we make the gray approximation, $\langle\langle T_{ph}\rangle\rangle = \langle\langle\lambda_{ph}\rangle\rangle/(L + \langle\langle\lambda_{ph}\rangle\rangle)$.

The value of 4/3 in Eq. (7a) comes from the difference between the MFP for scattering and the MFP for backscattering. The usual definition of mean-free-path is the average distance that a carrier travels before scattering. In the Landauer approach, $\lambda_{ph}(\omega)$ is the mean-free-path for backscattering and has a specific meaning; it is the length at which the transmission $T_{ph} = \lambda_{ph}(\omega)/(L + \lambda_{ph}(\omega))$ drops to one-half, and the inverse of the $\lambda_{ph}(\omega)$ is interpreted as the probability per unit length that a positive flux is converted into a negative flux. Following the proper definition of $\lambda_{ph}(\omega)$,[21] it can be shown that in 1D, $\lambda_{ph}(\omega) = 2l_{ph}(\omega)$, in 2D, $\lambda_{ph}(\omega) = (\pi/2)l_{ph}(\omega)$, and in 3D, $\lambda_{ph}(\omega) = (4/3)l_{ph}(\omega)$.

We have shown that the Landauer approach provides a simple but physically insightful description of diffusive transport, quasi-ballistic transport, and ballistic transport, but it does have limitations. For example, for problems like cross-plane thermal transport, we made the assumption of ideal contacts (i.e., that are reflection-less and that maintain a near-equilibrium thermal population of phonons). The role of contacts is problem-specific and should be considered on a case-by-case basis. Problems involving space and time dependent transport and multi-dimensional transport tend to be easier to handle with the Boltzmann equation, but for 1D, steady-state transport, the Landauer approach provides significantly more physical insight as well as computational advantages in computing the transport distribution (or number of channels, $M(\omega)$).

VI. SUMMARY AND CONCLUSION

In this paper, we showed that a simple Landauer model in the diffusive limit with a full phonon dispersion reproduces the results of more sophisticated molecular dynamics simulations of phonon transport in bulk Si. For thin Si films, the same approach also accurately describes the measured in-plane (diffusive transport) and cross-plane (quasi-ballistic transport) thermal conductivities, κ_{ph} vs. thickness of the Si layer. The spectral analysis of cumulative thermal conductivity as a function of a MFP demonstrates that the commonly used average MFP should be used with caution because it does not convey which phonons mainly contribute to the heat conduction. In the ballistic limit and with the Debye approximation, the Landauer model yields the Casimir limit, the blackbody radiation law for phonons. The results presented here shed new light on phonon transport in Si structures and also show that the Landauer approach provides a simple and useful computational approach that gives new insights into phonon transport from the ballistic to diffusive regimes in both nanostructures and bulk materials.

ACKNOWLEDGMENTS

This work was supported by MARCO Materials Structures and Devices (MSD) Focus Center and computational services were provided by the Network for Computational Nanotechnology (NCN). The authors also acknowledge illuminating discussions with N. Mingo, E. Pop, R. Venkatasubramanian, K. Goodson, A. M. Marconnet, and J. Maassen.

[1]H. B. G. Casimir, Physica **5**, 495–500 (1938).
[2]A. J. Minnich, M. S. Dresselhaus, Z. F. Ren, and G. Chen, Energy Environ. Sci. **2**, 466–479 (2009).
[3]J. Callaway, Phys. Rev. **113**, 1046 (1959).
[4]M. Asheghi, M. N. Touzelbaev, K. E. Goodson, Y. K. Leung, and S. S. Wong, J. Heat Transfer **120**, 30 (1998).
[5]M. Asheghi, Y. K. Leung, S. S. Wong, and K. E. Goodson, Appl. Phys. Lett. **71**, 1798–1800 (1997).
[6]Y. S. Ju and K. E. Goodson, Appl. Phys. Lett. **74**, 3005–3007 (1999).
[7]W. Liu and M. Asheghi, J. Appl. Phys. **98**, 123523 (2005).
[8]P. Chantrenne, J. L. Barrat, X. Blase, and J. D. Gale, J. Appl. Phys. **97**, 104318 (2005).
[9]Y. F Zhu, J. S Lian, and Q. Jiang, Appl. Phys. Lett. **92**, 113101 (2008).
[10]J. M Ziman, *Electrons and Phonons: The Theory of Transport Phenomena in Solids* (Oxford University Press, New York, 1960).
[11]M. Maldovan, J. Appl. Phys. **110**, 034308 (2011).
[12]P. E. Hopkins, C. M. Reinke, M. F. Su, R. H. Olsson, E. A. Shaner, Z. C. Leseman, J. R. Serrano, L. M. Phinney, and I. El-Kady, Nano Lett. **11**, 107–112 (2010).
[13]D. P. Sellan, E. S. Landry, J. E. Turney, A. J. H. McGaughey, and C. H. Amon, Phys. Rev. B **81**, 214305 (2010).
[14]D. P. Sellan, J. E. Turney, A. J. H. McGaughey, and C. H. Amon, J. Appl. Phys. **108**, 113524 (2010).
[15]A. J. H. McGaughey, E. S. Landry, D. P. Sellan, and C. H. Amon, Appl. Phys. Lett. **99**, 131904 (2011).
[16]A. Majumdar, ASME Trans. J. Heat Transfer **115**, 7–16 (1993).
[17]E. T. Swartz and R. O. Pohl, Rev. Mod. Phys. **61**, 605 (1989).
[18]S. Datta, *Electronic Transport in Mesoscopic Systems* (Cambridge University Press, 1997).
[19]D. E. Angelescu, M. C. Cross, and M. L. Roukes, Superlattices Microstruct. **23**, 673–689 (1998).
[20]N. Mingo, Phys. Rev. B **68**, 113308 (2003).
[21]C. Jeong, R. Kim, M. Luisier, S. Datta, and M. Lundstrom, J. Appl. Phys. **107**, 023707 (2010).
[22]C. Jeong, S. Datta, and M. Lundstrom, J. Appl. Phys. **109**, 073718 (2011).
[23]G. D. Mahan and J. O. Sofo, Proc. Natl. Acad. Sci. U.S.A. **93**, 7436–7439 (1996).
[24]J. Tersoff, Phys. Rev. B **39**, 5566 (1989).
[25]J. D. Gale and A. L. Rohl, Mol. Simul. **29**, 291–341 (2003).
[26]M. G. Holland, Phys. Rev. **132**, 2461 (1963).
[27]M. Asen-Palmer, K. Bartkowski, E. Gmelin, M. Cardona, A. P. Zhernov, A. V. Inyushkin, A. Taldenkov, V. I. Ozhogin, K. M. Itoh, and E. E. Haller, Phys. Rev. B **56**, 9431 (1997).
[28]P. G. Klemens, Proc. Phys. Soc. London **A68**, 1113 (1955).
[29]C. Dames and G. Chen, J. Appl. Phys. **95**, 682–693 (2004).
[30]E. H. Sondheimer, Adv. Phys. **1**, 1–42 (1952).
[31]W. P. Maszara, J. Electrochem. Soc. **138**, 341 (1991).